Published in final edited form as:
J Bone Miner Res. 2013 June ; 28(6): 1386–1398. doi:10.1002/jbmr.1881.

Tumor Localization and Biochemical Response to Cure in Tumor-Induced Osteomalacia

William H. Chong[1], **Panagiota Andreopoulou**[1,2], **Clara C. Chen**[3], **James Reynolds**[3], **Lori Guthrie**[1], **Marilyn Kelly**[1], **Rachel I. Gafni**[1], **Nisan Bhattacharyya**[1], **Alison M. Boyce**[1,4], **Diala El-Maouche**[1], **Diana Ovejero Crespo**[1], **Richard Sherry**[5], **Richard Chang**[3], **Felasfa M. Wodajo**[6], **Gad B. Kletter**[7], **Andrew Dwyer**[3], and **Michael T. Collins**[1]

[1]Skeletal Clinical Studies Unit, Craniofacial and Skeletal Disease Branch, National Institute of Dental and Craniofacial Research, National Institutes of Health, Bethesda, MD

[2]Division of Endocrinology, Department of Medicine, Einstein College of Medicine, Montefiore Medical Center, Bronx, NY 10461

[3]Nuclear Medicine, Radiology and Imaging Sciences, Hatfield Clinical Research Center, National Institutes of Health, Bethesda, MD

[4]Bone Health Program, Division of Orthopaedics and Sports Medicine, Children's National Medical Center, Washington, DC 20010

[5]Surgery Branch, Center for Cancer Research, National Cancer Institute, National Institutes of Health, Bethesda, MD

[6]Musculoskeletal Oncology, Virginia Hospital Center, Arlington, VA

[7]Pediatric Endocrinology, Swedish Pediatric Specialty Clinics, Swedish Hospital, Seattle, WA

Abstract

Tumor-induced osteomalacia (TIO) is a rare disorder of phosphate wasting due to fibroblast growth factor-23 (FGF23)-secreting tumors that are often difficult to locate. We present a systematic approach to tumor localization and post-operative biochemical changes in 31 subjects with TIO. All had failed either initial, or re-localization (in case of recurrence or metastases at outside institutions). Functional imaging with ^{111}Indium-octreotide with single photon emission computed tomography (octreo-SPECT or SPECT/CT), and ^{18}fluorodeoxyglucose positron emission tomography/CT (FDG-PET/CT) were performed, followed by anatomic imaging (CT,MRI). Selective venous sampling (VS) was performed when multiple suspicious lesions were identified or high surgical risk was a concern. Tumors were localized in 20/31 subjects (64.5%). Nineteen of 20 subjects underwent octreo-SPECT imaging, and 16/20 FDG-PET/CT imaging. Eighteen of 19 (95%) were positive on octreo-SPECT, and 14/16 (88%) on FDG-PET/CT. Twelve of 20 subjects underwent VS; 10/12 (83%) were positive. Sensitivity, specificity, positive predictive value (PPV), and negative predictive value (NPV) were: sensitivity=0.95, specificity=0.64, PPV=0.82 and NPV=0.88 for octreo-SPECT; sensitivity=0.88, specificity=0.36, PPV=0.62 and NPV=0.50 for FDG-PET/CT. Fifteen subjects had their tumor resected at our institution, and were disease-free at last follow-up. Serum phosphorus returned to normal in all subjects within 1-5 days. In 10 subjects who were followed for at least 7 days postoperatively, intact FGF23 (iFGF23) decreased to near undetectable within hours and returned to the normal range within 5 days. C-terminal FGF23 (cFGF23) decreased immediately but remained elevated, yielding a markedly elevated cFGF23/iFGF23 ratio. Serum 1,25-dihydroxyvitamin D_3 (1,25D) rose and exceeded the normal range. In this systematic approach to TIO tumor localization Octreo-SPECT was more sensitive and specific, but in many cases FDG-PET/CT was complementary. VS can discriminate between multiple suspicious lesions and increase certainty prior to surgery.

Sustained elevations in cFGF23 and 1,25D were observed, suggesting novel regulation of FGF23 processing and 1,25D generation.

Keywords

FGF23; hypophosphatemia; mineral metabolism; vitamin D

Introduction

Tumor-induced osteomalacia (TIO) is a rare paraneoplastic disorder in which over-production of fibroblast growth factor-23 (FGF23) by small mesenchymal tumors leads to renal phosphate wasting, low 1,25-dihydroxyvitamin D_3 (1,25-D), hypophosphatemia and osteomalacia (1-3). Subjects often present with generalized and non-specific symptoms of bone pain, muscle aches and weakness. As phosphorus may not be routinely measured and/or further evaluation of hypophosphatemia may not be pursued, patients often go undiagnosed for many years.

The diagnosis of TIO is suspected when patients with hypophosphatemia are shown to have low tubular reabsorption of phosphate (TRP), low or inappropriately normal 1,25-D and elevated FGF23. TIO is confirmed when these resolve after tumor resection. Other FGF23-mediated diseases that cause hypophosphatemia, such as X-linked hypophosphatemic rickets, and autosomal dominant and recessive hypophosphatemic rickets, need to be excluded, especially in younger patients and in patients with a family history of hypophosphatemia. Since complete surgical excision of culprit tumors leads to cure of the disease, diagnosing TIO and successfully locating a causative tumor is of utmost importance.

Tumors responsible for TIO are typically small mesenchymal tumors that can be located in nearly every part of the body (1,2,4). Difficulty in localizing these tumors further delays definitive therapy for many patients. Multiple types of localizing studies have been used with mixed results (5-13). We report here a large series and discuss a systematic approach to localizing these rare tumors. In addition, to further investigate the role of FGF23 on mineral metabolism we measured the serum levels of serum phosphorus, intact FGF23 (iFGF23), C-terminal FGF23) cFGF23, and 1,25-D following surgical cure.

Methods

Thirty-one subjects (20 male, 11 female) with TIO were seen between October 1998 and June 2012 (Table 1). All subjects were initially seen at other institutions where they had undergone failed attempts at tumor localization (often multiple), either at the initial presentation, after recurrence, or after what was found to be metastases. Subject ages ranged from 14 to 67 years of age at time of presentation to NIH (mean 48.5, median 47). All subjects had the typical biochemical features of hypophosphatemia and elevated levels of iFGF23. The TIO-related skeletal complications are listed in Table 1. Three subjects underwent iliac crest biopsies that were embedded in plastic and assessed for the presence of osteomalacia. All subjects had clear evidence of osteomalacia (not shown). Other causes of FGF23-mediated hypophosphatemia were excluded when necessary by detailed family history and/or genetic testing, as indicated. In this series, the two subjects under 18 years of age had genetic testing for X-linked, autosomal dominant and autosomal recessive hypophosphatemic rickets. In addition, all of the adult subjects in whom a tumor was not identified had genetic testing performed for X-linked and autosomal recessive

hypophosphatemic rickets. No mutations were identified. Subject records were reviewed for biochemical data, results of imaging studies and outcomes of treatment.

Plasma iFGF23 was measured using a commercially available ELISA assay that detects only iFGF23 (Kainos, Tokyo, Japan). Plasma cFGF23 was measured using a commercially available ELISA assay that detects both iFGF23 and cFGF23 (Immutopics, San Clemente, CA). Under most physiologic circumstances iFGF23 and cFGF23 levels are in a 1:1 ratio as determined by these assays, and differences between iFGF23 and cFGF23 levels are thought to reflect cFGF23 fragments derived from iFGF23 degradation/metabolism (14). Other mineral metabolism analytes were determined by commercially available assays.

A multi-modality approach was used to localize tumors. Functional imaging studies included whole body (including head and extremities) ^{111}In-octreotide with single photon emission computed tomography (octreo-SPECT, octreo-SPECT/CT was available from May, 2008 on), whole body (including head and extremities) ^{18}fluorodeoxyglucose positron emission tomography/computed tomography (FDG-PET/CT), ^{99}Tc-bone scintigraphy (bone scans), and ^{99}Tc-sestamibi scans (MIBI). Anatomic imaging of suspicious areas identified on functional studies was performed with CT and MRI. Venous sampling (VS) was performed for one of three indications: 1) identification of multiple suspicious lesions requiring confirmation of the true positive lesion 2) need for increased certainty that a lesion was the culprit tumor and 3) a subject was a positive control in an earlier study examining the utility of venous sampling (13). Increased certainty was needed when surgical resection was associated with a potential high risk of morbidity, or when other localizing studies were not completely convincing. Subjects in whom a putative causative tumor was identified underwent surgical resection.

Ten subjects were monitored for biochemical response to successful tumor resection for at least 7 days.

Results

Tumor localization

Using a systematic and multi-modal approach to localization, the causative tumor was located in 20 of 31 subjects (64.5%). Locations are indicated in Figure 1.

Functional imaging studies

A combination of nuclear imaging studies was used in an attempt to localize culprit tumors. Early in our experience, subjects were imaged with octreo-SPECT, FDG-PET/CT, MIBI and bone scans. As more experience was gained, MIBI and bone scans were abandoned as neither of these imaging modalities offered additional utility compared to the combination of octreo-SPECT and FDG-PET/CT.

Octreo-SPECT imaging was performed in 30 of 31 subjects. Nineteen of 20 subjects in whom a tumor was successfully identified underwent octreo-SPECT imaging. The one subject who did not have octreo-SPECT imaging had resection of a causative subcutaneous tumor prior to the study. Seventeen of 19 (90%) of these studies identified lesions that were ultimately found to be the causative tumor. The 11 subjects in whom no causative tumor was found had octreo-SPECT imaging. Four (36%) of these studies showed suspicious areas which were further evaluated but ultimately found not to be the tumor (false positive). Tumor was excluded by a combination of negative anatomical imaging (CT and/or MRI), and/or negative venous sampling as evidenced by a tumor bed/general circulation FGF23 ratio < 1.7 (13).

FDG-PET/CT was performed in 27 of 31 (87%) subjects. Sixteen of 20 subjects in whom a tumor was successfully identified had FDG-PET/CT. Fourteen of these studies identified suspicious lesions which included the causative tumor (88%). Of the 2 subjects with negative FDG-PET/CT studies, 1 subject was subsequently found to have an intracranial lesion which made identifying the lesion by FDG-PET/CT impossible due to high glucose uptake by the brain. All 11 subjects in whom no causative tumor was found had FDG-PET/CT. Five (45%) of these studies showed suspicious areas which were further evaluated but ultimately found not to be the tumor (false positive).

Sensitivity, specificity, positive predictive value (PPV), and negative predictive value (NPV) calculations yielded sensitivity = 0.95, specificity = 0.64, PPV = 0.82 and NPV = 0.88 for octreo-SPECT; and sensitivity = 0.88, specificity = 0.36, PPV = 0.62 and NPV = 0.50 for FDG-PET/CT (Table 2). While octreo-SPECT was the superior single study, in 7/20 (35%) subjects, FDG-PET/CT imaging was useful or necessary in the initial identification of the tumor and/or confirming a lesion on octreo-SPECT imaging This reflects complementarity between the two studies and the utility of performing both studies in many cases.

Anatomic Imaging

Following identification of suspicious lesions on nuclear imaging studies, CT and MRI of the region of interest were performed to confirm that the presumptive lesion had features consistent with a tumor. In cases where no suspicious lesions were identified by functional imaging, anatomic imaging was performed to evaluate areas poorly seen on functional imaging (brain, liver, and spleen). In addition areas thought to be more likely to harbor tumors based on previous reports also underwent anatomical imaging (sinuses and extremities). Anatomic imaging without positive functional imaging was performed in 4 subjects (subjects 8, 17, 20, 25). In none of these subjects was a tumor identified. Of the 11 subjects in whom a tumor was never found, functional imaging identified suspicious area in 6 (subjects 4, 7, 9, 18, 24, 27). Further evaluation of these areas failed to identify a causative tumor; these were considered false positive functional imaging studies. One subject did not complete the evaluations (subject 12). One subject (subject 20) was found to have a suspicious lesion on anatomic imaging with negative functional imaging. Resection of this lesion however did not result in cure. In the eleven subjects in whom a tumor was not identified, a causative tumor was excluded by a combination of anatomic imaging, venous sampling, or surgery.

Selective venous sampling

Of the 20 subjects in whom the culprit tumor was found, 13 underwent VS. Eleven of thirteen (85%) of these successfully localized the tumor by demonstrating a gradient of > 1.7 in the level of FGF23 near the tumor compared to peripheral venous samples. The gradient of 1.7 had been previously established in a study evaluating VS in TIO (13). In 1 of 2 unsuccessful venous sampling studies (subject 1), the study was performed to evaluate for persistent/recurrent disease (subject 1). In subject 14, a lesion in the vertebral body was identified on both anatomical and functional imaging and the subject underwent venous sampling for confirmation. However, probably due to the vagaries of the venous anatomy around the spine, VS was negative. A fine needle aspiration biopsy of the suspicious lesion confirmed the tumor on the basis of cytology and FGF23 measurement of washings (aspirate 1140 pg/mL, peripheral circulation 157 pg/mL). Of the 11 subjects in whom no causative tumor was found, VS was performed in 6. Two of these cases (subjects 18 and 20) demonstrated an increase in FGF23 levels at a single site suggestive of tumor, but resection of the suspicious area did not lead to resolution of disease and no phosphaturic tumor was identified in the resected material. No VS studies suggested more than a single anatomical site. Values showed either elevations anatomically adjacent to each other, or, in the case of

negative studies, values with a normal distribution, probably reflecting assay and physiologic variation and inconsistent with the identification of site of tumor.

Tumor Locations

Causative tumors were identified throughout the body. Four tumors occurred in the head and neck, 14 occurred in the extremities and 2 were located in the torso. Ten tumors were located in soft tissue and 9 were in bone. Both subjects who developed metastases had metastatic disease to the lung. A summary of tumor locations and results of localizing studies is provided in Table 3 and Fig. 1.

Outcomes

Of the 20 subjects in whom a tumor was found, 19 subjects had surgical resection of the tumor. One subject (subject 22) refused surgery and was treated with radiation therapy. Subjects 2, 6 and 10 had the initial resection prior to referral to our institution. Three subjects (1, 2 and 6) developed persistent/recurrent disease. Subject 1 is believed to have persistent/recurrent disease at the site of the original tumor, as the tumor margins of the resected tissue were positive for tumor and no distant metastases have been detected. However, VS from the region was negative and biopsies of the previous surgical site did not reveal tumor. She remains with mild, but persistent disease on medical therapy 12 years after the initial resection. Subject 2 presented in childhood with rickets and had the initial resection as well as multiple resections for recurrent disease prior to referral to our institution. She was referred to our institution for further evaluation of recurrent disease. The diagnosis was confirmed and pulmonary metastases were identified as the cause. She underwent multiple metatasetectomies. Improvement in disease with resection and FGF23 staining of the tumors confirmed pulmonary metastases as the cause of her disease. She underwent resection of metastases and participated in a trial of inhaled chemotherapeutic agents in an attempt to control the disease but ultimately died from disease-related complications. Subject 6 has had resection of recurrent disease at the site of the original tumor, but eventually was found to have pulmonary metastases. He is currently on medical therapy that includes cinacalcet (15,16). The remaining subjects have shown no evidence of recurrent disease at last follow-up (1-12 years).

Four subjects underwent surgical resection of a suspicious lesion thought to be the causative tumor without resolution of disease (subjects 4, 7, 18 and 20). The histopathological findings were not consistent with a phosphaturic tumor and the blood phosphorus and FGF23 levels did not change postoperatively. These subjects along with other subjects in whom a causative tumor was not identified have been managed medically with phosphorus supplementation, active vitamin D analogs, and as indicated, cinacalcet.

A group of 14 subjects whose tumor was resected had alkaline phosphatase levels measured for an extended period postoperatively. In all subjects alkaline phosphatase levels were elevated at presentation (mean ± 1 SD 315 ± 176 U/L, median 240, range 113-692, normal range 37-116). The degree of elevation paralleled disease severity, but was impacted by whether or not a subject was treated with phosphate supplementation prior to presentation. In no subjects was there a significant change within the first two weeks post-surgery, but in all subjects but one the level returned to normal by 12 months (data not shown).

Ten subjects had blood levels of mineral metabolites monitored for at least 7 days postoperatively (Fig. 2). At the time of surgery and in the postoperative period, no subjects were taking phosphorus or calcitriol supplements, and all subjects had a 25 hydroxy vitamin D level of at least 25 ng/ml. The average serum phosphorus was normal by day 2, and in all subjects it was normal by day 5 (Fig. 2A). Plasma iFGF23 levels dropped precipitously,

usually within hours, and did not return to normal in all subjects monitored until postoperative day 10 (Fig. 2B). Interestingly, while cFGF23 also dropped rapidly, in the majority of cases the blood level did not fall into the normal range, achieved a new and elevated steady state, and remained elevated throughout the period monitored (Fig. 2C). As a consequence, the cFGF23/iFGF23, which was approximately 1 at baseline, increased and was elevated throughout the period of monitoring (Fig. 2D). Serum 1,25-D levels were low at the time of surgery and began to rise in the postoperative period (Fig. 2E). Levels were markedly elevated above the normal range from postoperative day 3 onward, and began to decline by day 10. Average PTH levels were elevated for the first several days following surgery and then normalized (Fig. 2F). The elevation in average PTH levels was driven by one subject. All other subjects had normal PTH values. Mean blood calcium levels were normal throughout the observation period (Fig. 2G).

The tumor has not been found in any of the subjects listed in the “Not Localized” section of Table 3. The range of follow-up for this group was from 2-9 years. Subjects had between 3-5 rounds of attempts at localization, with usually at least one year between rounds of localizing studies. One subject was lost to follow-up and one subject died from complications due to liver failure, presumably unrelated to TIO.

Discussion

TIO can be a devastating disease leading to pain, fractures, functional impairment, and weakness. Difficulty localizing these tumors often limits the ability to provide definitive surgical therapy. Causative tumors are typically very small and can occur in locations sometimes not included in the standard field of FDG-PET/CT and/or octreo-SPECT studies. When located, complete surgical resection results in a dramatic resolution of symptoms and cure of disease.

We have found that a systematic approach to tumor localization allows for improved success in tumor localization. Octreo-SPECT provided the best combination of sensitivity and specificity and is therefore the best initial study. The addition of FDG-PET/CT can be considered if no lesion or multiple lesions are identified on octreo-SPECT. In cases when no lesions are identified on octreo-SPECT, FDG-PET/CT can suggest a lesion that was initially missed on the octreo-SPECT. An example of this complementarity is demonstrated in Figure 3. Anatomic imaging is used to confirm the presence of a tumor after suspicious lesions have been identified on functional imaging. When multiple suspicious lesions are identified on functional and anatomical imaging, VS can be used to discriminate between false and true positive lesions. The case presented in Figure 4 is a representative example. VS can also be used to increase diagnostic certainty when the resection of the presumed tumor may be associated with significant morbidity and the surgeon, physician, or patient would like greater assurance that the lesion being excised is the culprit and that resection will result in cure. The FGF23 assay used in the VS studies shown here involved the use of intact FGF23 assay (Kainos, Tokyo, Japan), which may have greater sensitivity and specificity than the assay that is available in commercial laboratories (Immutopics, San Clemente, CA), but in most cases the Immutopics assay would presumably provide adequate diagnostic ability. In the setting of multiple lesions seen on either octreo-SPECT or FDG-PET/CT, careful side-by-side comparison of both studies allows for identification of lesions that co-register and are thus more likely to be the causative tumor. The approach outlined above is detailed in Figure 5.

Jiang et al. recently described their experience in a large series of subjects with TIO (17). The tumor was found in only 40/94 (42%) of the subjects. This is significantly less than the 20/31 (65%) in this series. This most likely reflects the reliance upon a single imaging

modality, octreo-SPECT, which was used in this series of patients, and further supports the approach outlined here (Fig. 5).

Another point to emphasize in the evaluation of these subjects is the need for whole body imaging. Tumors can occur in locations not typically visualized on the standard field of octreo-SPECT or FDG-PET/CT. In fact, in two subjects in this series (subjects # 6 and 30) the tumor was not identified at the outside institution because the site of the tumor was not included in the field of either the octreo-SPECT or the FDG-PET/CT (18).

Four of the 11 subjects in whom the tumor was not found underwent surgery based upon what were false positive findings on localizing studies. In all cases, either FDG-PET/CT or octreo-SPECT gave false positive findings, but in no cases did the false positive FDG-PET/CT and octreo-SPECT lesions co-register. It was in part these four failures that contributed to the recommendation that co-registration be a requirement for proceeding to surgery. The one false negative VS study was attributed to the fact the tumor was in an anatomical location with complicated venous drainage, the para-vertebral area. In this case, diagnostic certainty was achieved by a needle biopsy of the lesion with FGF23 measurement of the aspirate washings and by cytology. Experience with this technique, however, is limited and risk of tumor seeding is as yet unknown and may be a concern.

Anatomic imaging of suspicious regions with CT and/or MRI was performed but no common or specific features were noted. Just as these are a heterogeneous group of tumors in location, tissue type, and pathologic description, the CT/MRI characteristics are also heterogeneous. The lack of specific or typical suspicious features along with the frequency of incidental findings of unknown significance suggests that blind anatomic imaging is of limited benefit. In all cases in which the tumor was visualized on anatomical imaging, it had been guided by functional imaging.

An interesting postoperative finding was the sustained elevation in cFGF23 levels (resulting in an increased cFGF23/iFGF23). The elevated cFGF23 levels and increased cFGF23/iFGF23 ratio observed postoperatively may reflect an alteration in FGF23 processing; a phenomenon that has recently been identified as a regulated process and that may be of clinical significance (14). While speculative, one possible explanation for this observation is that removal of the tumor and rapid clearance of iFGF23 from the circulation unmasks the production of cFGF23 produced by osteocytic cleavage of iFGF23. An alternative explanation is that cFGF23 undergoes clearance from the circulation much more slowly than iFGF23 and that this is reflected in the sustained cFGF23 levels observed. This is unlikely given that the data would represent a terminal half-life of cFGF23 greater than 10 days, and that even in renal failure there is no cFGF23 observed in the circulation (19).

An additional interesting postoperative finding was the marked and sustained rise in 1,25-D. The findings are not likely explained by perturbation in the levels of the established regulators of renal 1-α hydroxylase, which converts 25-hydroxyvitamin D to 1,25-D, and it is probably different from the prolonged elevation that has been reported in alkaline phosphatase after tumor removal (20). In all but one subject PTH was normal, serum FGF23 had returned to normal, and serum phosphorus and calcium had also returned to normal. Therefore, neither serum PTH, FGF23, phosphorus, or calcium explains the sustained elevation in serum 1,25D. Here too tumor removal appears to have unmasked recovery from 1-hydrxylase FGF23-mediated suppression via an as yet unidentified mechanism.

Conclusions

A systematic approach to tumor localization for the patient with TIO is essential. After excluding other potential diagnoses, patients should first be assessed with a thorough

physical examination, including the oropharynx. Whole body functional imaging with octreo-SPECT should be performed first, followed by FDG-PET/CT if a clear single candidate lesion is not identified on octreo-SPECT. As the findings can be very subtle, and there may be multiple regions of interest, it is advisable to review the studies in-person with the nuclear medicine physician. Anatomic imaging should follow to confirm a possible tumor. In situations where multiple highly suspicious lesions are found, or if the lesion is located in an area where high surgical morbidity is anticipated, VS should be performed to increase confidence of tumor location prior to surgery. Once a causative tumor is found, surgical resection with wide margins to insure complete resection should be the treatment of choice. The elevations in cFGF23 and 1,25D observed after tumor removal suggest previously unexplained regulation of both FGF23 processing at the level of the bone and 1,25D generation at the kidney.

Acknowledgments

This research was supported by the Intramural Research Program of the NIH, NIDCR

References

1. Chong WH, Molinolo AA, Chen CC, Collins MT. Tumor-induced osteomalacia. Endocrine-related cancer. 2011; 18(3):R53–77. [PubMed: 21490240]
2. Jan de Beur SM. Tumor-induced osteomalacia. Jama. 2005; 294(10):1260–1267. [PubMed: 16160135]
3. Drezner MK. Tumor-induced osteomalacia. Rev Endocr Metab Disord. 2001; 2(2):175–186. [PubMed: 11705323]
4. Folpe AL, Fanburg-Smith JC, Billings SD, Bisceglia M, Bertoni F, Cho JY, Econs MJ, Inwards CY, Jan de Beur SM, Mentzel T, Montgomery E, Michal M, Miettinen M, Mills SE, Reith JD, O'Connell JX, Rosenberg AE, Rubin BP, Sweet DE, Vinh TN, Wold LE, Wehrli BM, White KE, Zaino RJ, Weiss SW. Most osteomalacia-associated mesenchymal tumors are a single histopathologic entity: an analysis of 32 cases and a comprehensive review of the literature. Am J Surg Pathol. 2004; 28(1):1–30. [PubMed: 14707860]
5. Duet M, Kerkeni S, Sfar R, Bazille C, Liote F, Orcel P. Clinical impact of somatostatin receptor scintigraphy in the management of tumor-induced osteomalacia. Clin Nucl Med. 2008; 33(11):752–756. [PubMed: 18936605]
6. Dupond JL, Mahammedi H, Magy N, Blagosklonov O, Meaux-Ruault N, Kantelip B. Detection of a mesenchymal tumor responsible for hypophosphatemic osteomalacia using FDG-PET. Eur J Intern Med. 2005; 16(6):445–446. [PubMed: 16198908]
7. Hesse E, Moessinger E, Rosenthal H, Laenger F, Brabant G, Petrich T, Gratz KF, Bastian L. Oncogenic osteomalacia: exact tumor localization by co-registration of positron emission and computed tomography. J Bone Miner Res. 2007; 22(1):158–162. [PubMed: 17014386]
8. von Falck C, Rodt T, Rosenthal H, Langer F, Goesling T, Knapp WH, Galanski M. (68)Ga-DOTANOC PET/CT for the detection of a mesenchymal tumor causing oncogenic osteomalacia. Eur J Nucl Med Mol Imaging. 2008; 35(5):1034. [PubMed: 18369618]
9. Kimizuka T, Ozaki Y, Sumi Y. Usefulness of 201Tl and 99mTc MIBI scintigraphy in a case of oncogenic osteomalacia. Ann Nucl Med. 2004; 18(1):63–67. [PubMed: 15072186]
10. Lee HK, Sung WW, Solodnik P, Shimshi M. Bone scan in tumor-induced osteomalacia. J Nucl Med. 1995; 36(2):247–249. [PubMed: 7830124]
11. Dissanayake AM, Wilson JL, Holdaway IM, Reid IR. Oncogenic osteomalacia: culprit tumour detection whole body magnetic resonance imaging. Intern Med J. 2003; 33(12):615–616. [PubMed: 14656239]
12. Nasu T, Kurisu S, Matsuno S, Tatsumi K, Kakimoto T, Kobayashi M, Nakano Y, Wakasaki H, Furuta H, Nishi M, Sasaki H, Suzuki H, Ito N, Fukumoto S, Nanjo K. Tumor-induced hypophosphatemic osteomalacia diagnosed by the combinatory procedures of magnetic resonance

imaging and venous sampling for FGF23. Internal medicine (Tokyo, Japan). 2008; 47(10):957–961.

13. Andreopoulou P, Dumitrescu CE, Kelly MH, Brillante BA, Cutler Peck CM, Wodajo FM, Chang R, Collins MT. Selective venous catheterization for the localization of phosphaturic mesenchymal tumors. J Bone Miner Res. 2011; 26(6):1295–1302. [PubMed: 21611969]
14. Bhattacharyya N, Wiench M, Dumitrescu C, Connolly BM, Bugge TH, Patel HV, Gafni RI, Cherman N, Cho M, Hager GL, Collins MT. Mechanism of FGF23 processing in fibrous dysplasia. J Bone Miner Res. 2012; 27(5):1132–1141. [PubMed: 22247037]
15. Bergwitz C, Collins MT, Kamath RS, Rosenberg AE. Case records of the Massachusetts General Hospital. Case 33-2011. A 56-year-old man with hypophosphatemia. N Engl J Med. 2011; 365(17):1625–1635. [PubMed: 22029985]
16. Geller JL, Khosravi A, Kelly MH, Riminucci M, Adams JS, Collins MT. Cinacalcet in the management of tumor-induced osteomalacia. J Bone Miner Res. 2007; 22(6):931–937. [PubMed: 17352646]
17. Jiang Y, Xia WB, Xing XP, Silva BC, Li M, Wang O, Zhang HB, Li F, Jing HL, Zhong DR, Jin J, Gao P, Zhou L, Qi F, Yu W, Bilezikian JP, Meng XW. Tumor-induced osteomalacia: an important cause of adult-onset hypophosphatemic osteomalacia in China: Report of 39 cases and review of the literature. J Bone Miner Res. 2012; 27(9):1967–1975. [PubMed: 22532501]
18. Chong WH, Yavuz S, Patel SM, Chen CC, Collins MT. The importance of whole body imaging in tumor-induced osteomalacia. J Clin Endocrinol Metab. 2011; 96(12):3599–3600. [PubMed: 22143830]
19. Shimada T, Urakawa I, Isakova T, Yamazaki Y, Epstein M, Wesseling-Perry K, Wolf M, Salusky IB, Juppner H. Circulating fibroblast growth factor 23 in patients with end-stage renal disease treated by peritoneal dialysis is intact and biologically active. J Clin Endocrinol Metab. 2010; 95(2):578–585. [PubMed: 19965919]
20. Shane E, Parisien M, Henderson JE, Dempster DW, Feldman F, Hardy MA, Tohme JF, Karaplis AC, Clemens TL. Tumor-induced osteomalacia: clinical and basic studies. J Bone Miner Res. 1997; 12(9):1502–1511. [PubMed: 9286768]

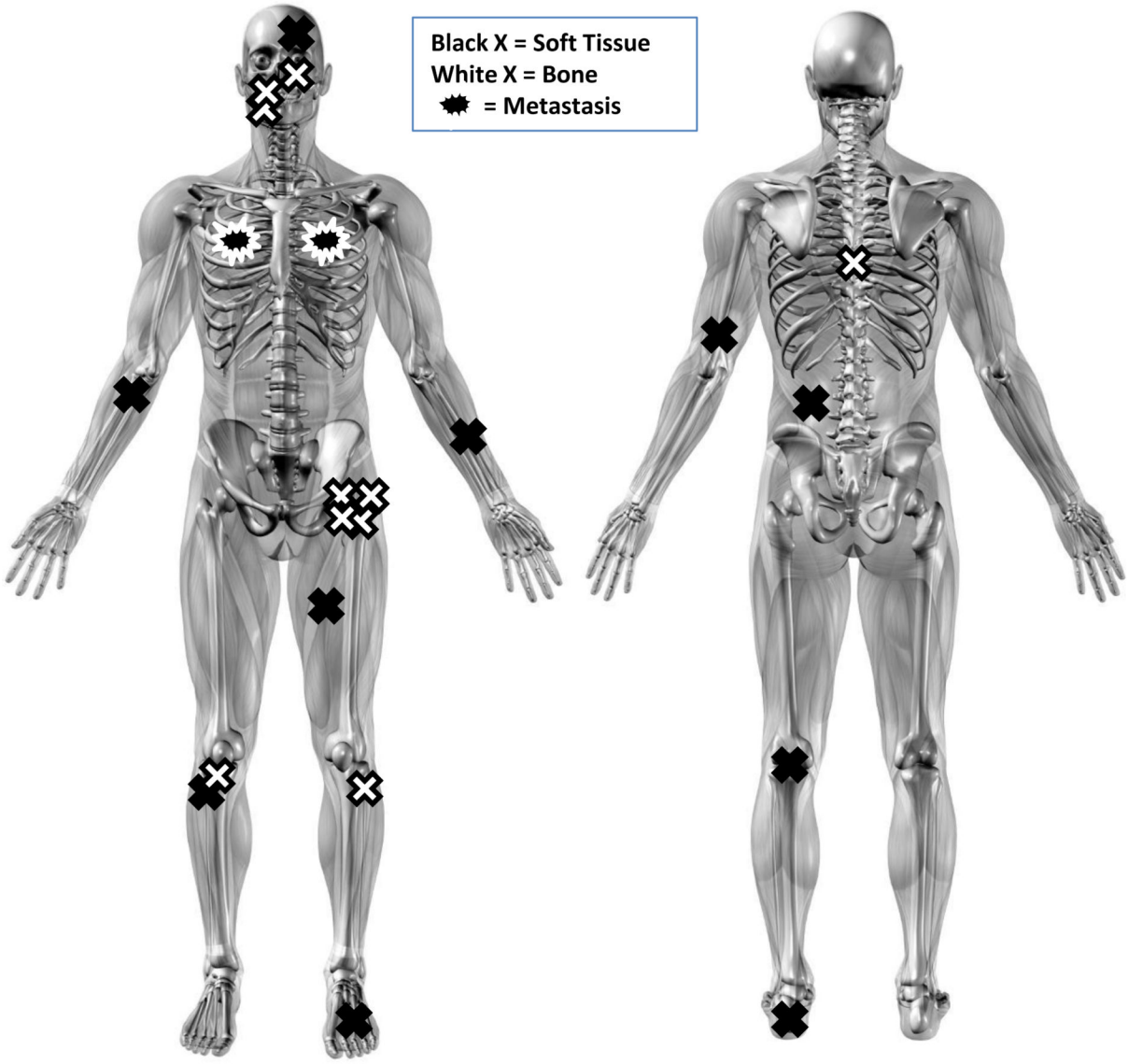

Figure 1.

Anatomical location of the 20 localized tumors confirmed to be causing tumor-induced osteomalacia. Black X's represent tumors located in soft tissues (10/20, 50%); white X's represent tumors located in bone (10/20, 50%). Star-like structures represents metastases. Four tumors occurred in the head and neck, 14 occurred in the extremities, and 2 occurred in the torso. Two subjects had metastases, both of which occurred in the lungs. One originated in the left forearm and the other arose from the right mandible. Fourteen of the 20 tumors were found on the left side of the body, 5 were found on the right side, and one was midline.

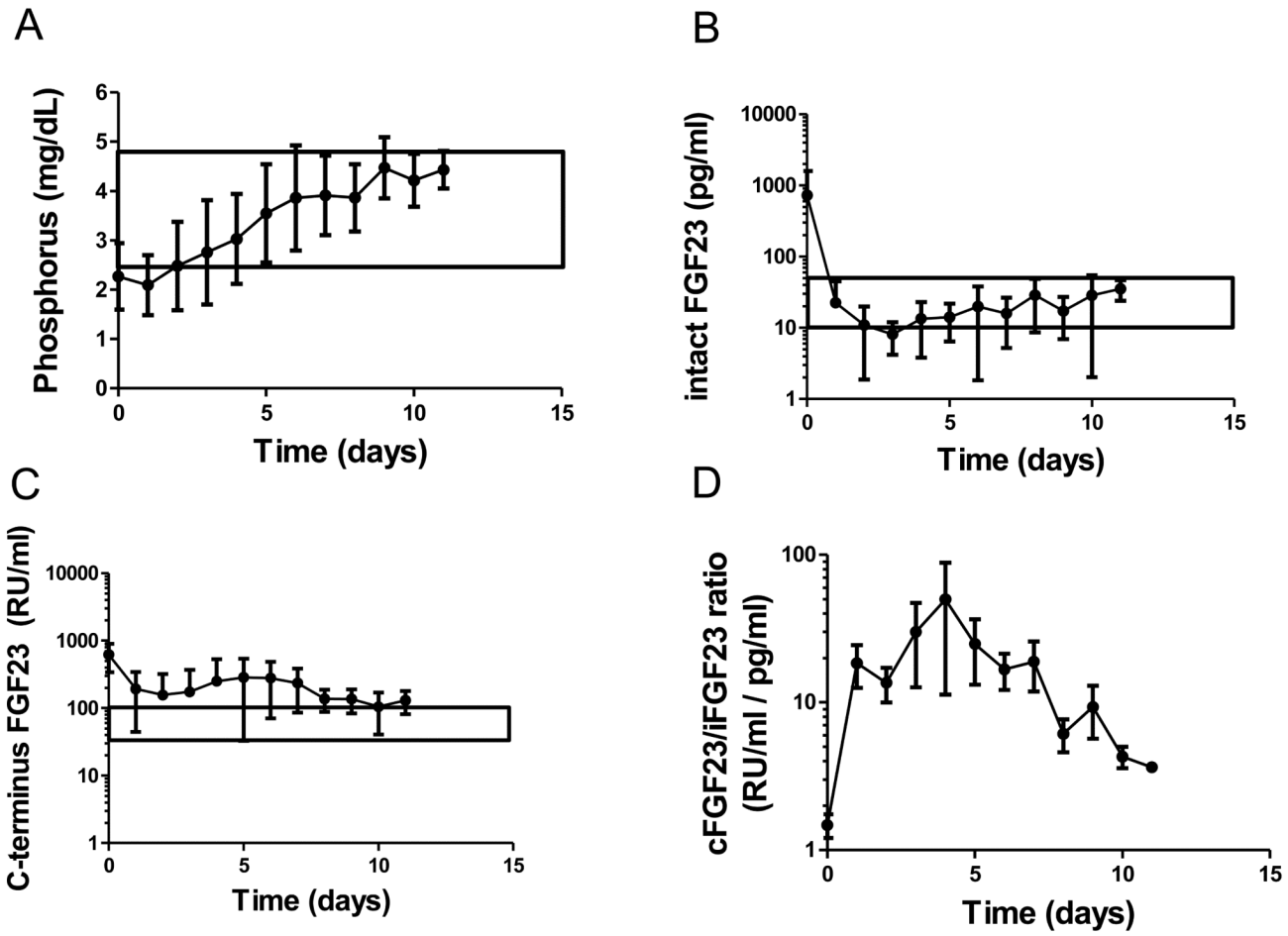

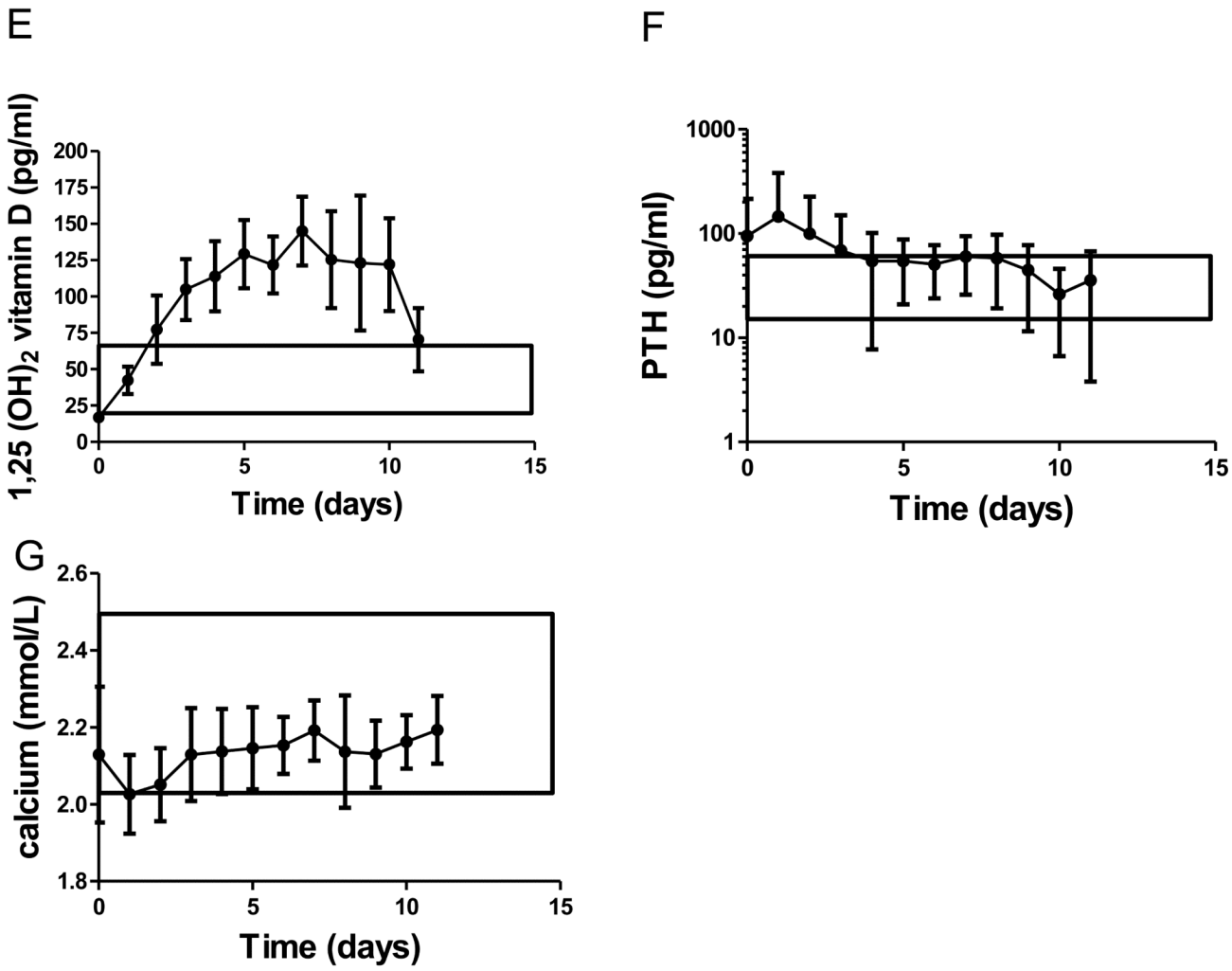

Figure 2.

Mineral metabolism after tumor resection: Levels of various measures of mineral metabolism were determined in ten subjects for up to 11 days after tumor resection. Blood was drawn at 8 am after an overnight fast. The mean serum phosphorus was normal by day 5 and in all subjects it was normal by day 7 (A). Plasma iFGF23 decreased rapidly after tumor resection, but did not return to normal in all subjects until day 11 (B). Plasma cFGF23 declined (but not into the normal range) and remained elevated post-operatively (C). As a consequence, the cFGF23/iFGF23 ratio was markedly increased and remained elevated throughout the period of monitoring (D). 1,25-dihydroxyvitamin D_3 began to rise immediately postoperatively, and was significantly elevated above the normal range during most of the postoperative period (E). Average PTH levels were elevated for the first several days following surgery then normalized (F). The elevation in the average PTH values were driven by very high levels in one subject (number 28) who was eventually found to have tertiary hyperparathyroidism and whose PTH values were quite elevated (at baseline 400-600 pg/ml). The PTH values in all other subjects were normal. Mean blood calcium levels were normal throughout the observation period (G). The normal ranges are indicated by the boxed areas.

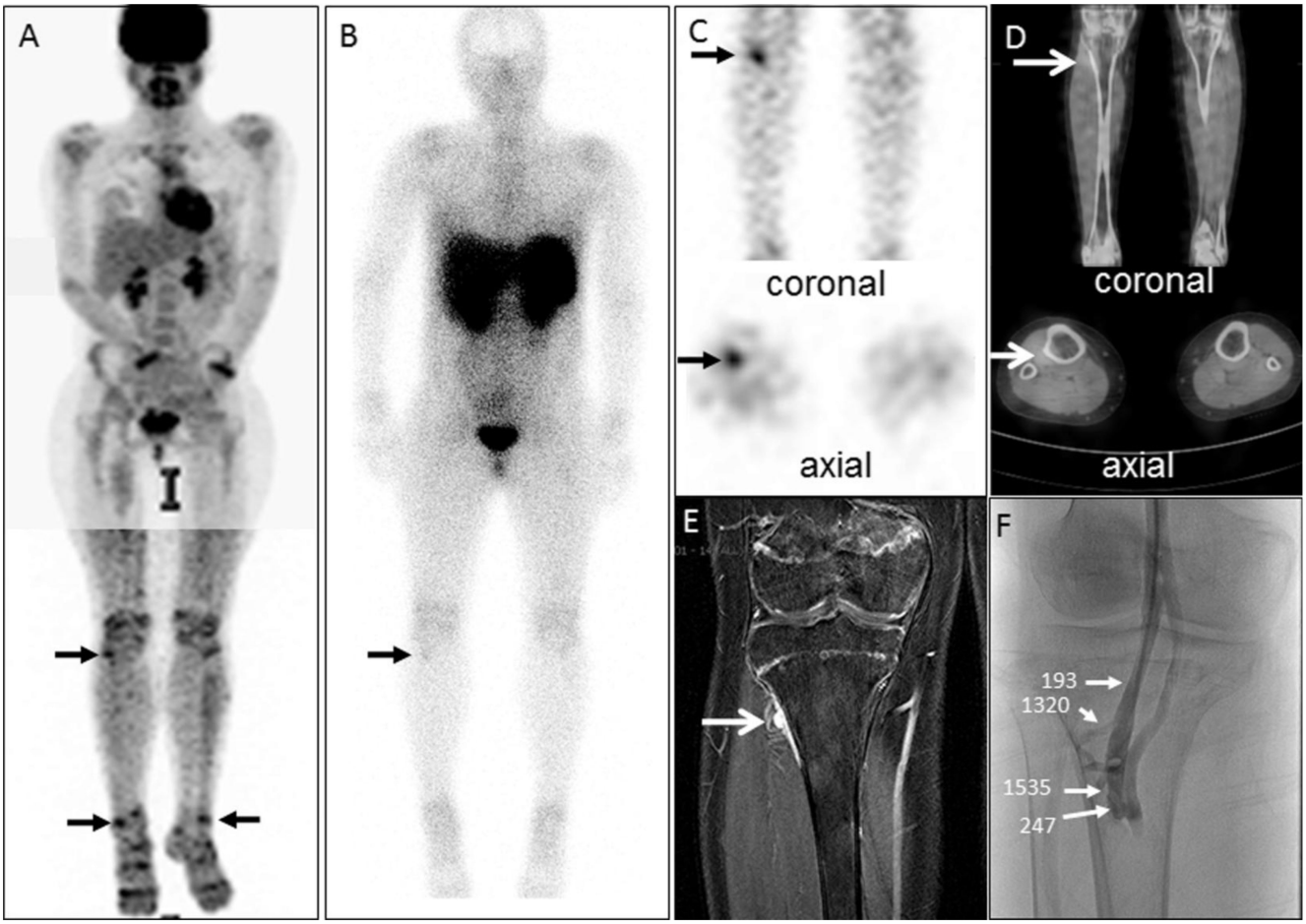

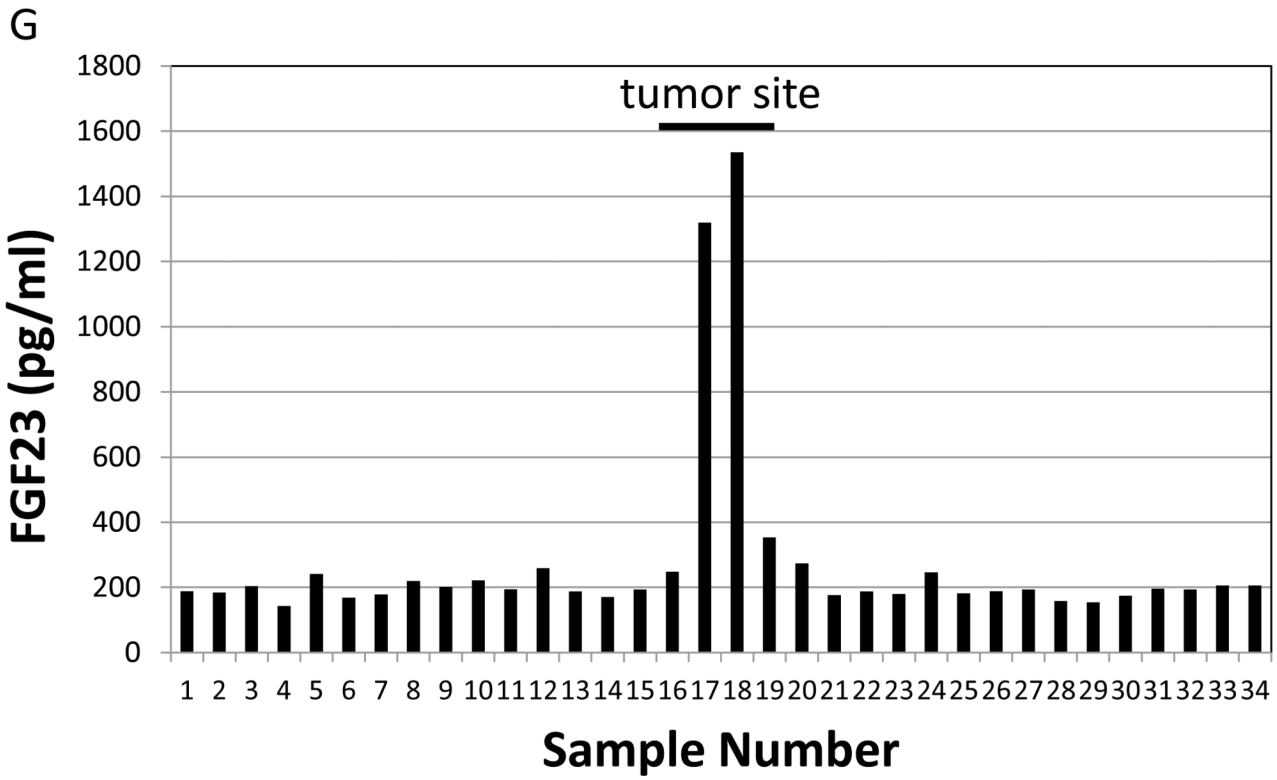

Figure 3.

An example of a case illustrating octreo-SPECT/CT and FDG-PET/CT complementarity: A 15-year-old girl who was found to have tumor-induced osteomalacia had an FDG-PET/CT study that demonstrated many areas of physiologic (e.g., brain, heart, kidneys) and non-physiologic (e.g., arrows) uptake (A). Subsequently an octreo-SPECT/CT study was performed that initially was read as negative (B). Guided by the non-physiologic FDG-PET/CT findings, a reevaluation of the octreo-SPECT/CT identified a suspicious lesion on the lateral aspect of the proximal right tibia on SPECT (C) and fused SPECT/CT (D) images (arrows). In retrospect the lesion was evident on the whole body image (B, arrow). Anatomic imaging identified a tumor on MRI (E). Further confirmation was deemed necessary prior to surgical resection, so venous sampling (VS) was performed. VS revealed a clear step-up in the region of the tumor suggested by functional and anatomical imaging (F&G). In panel F, the values indicate the intact FGF23 concentration at the location indicated by the arrows. In panel G, values from sites sampled are shown. The peripheral value was 188 pg/ml and the values at sites adjacent to the lesion were 1320 and 1535 pg/ml. The lesion was resected and the subject was cured.

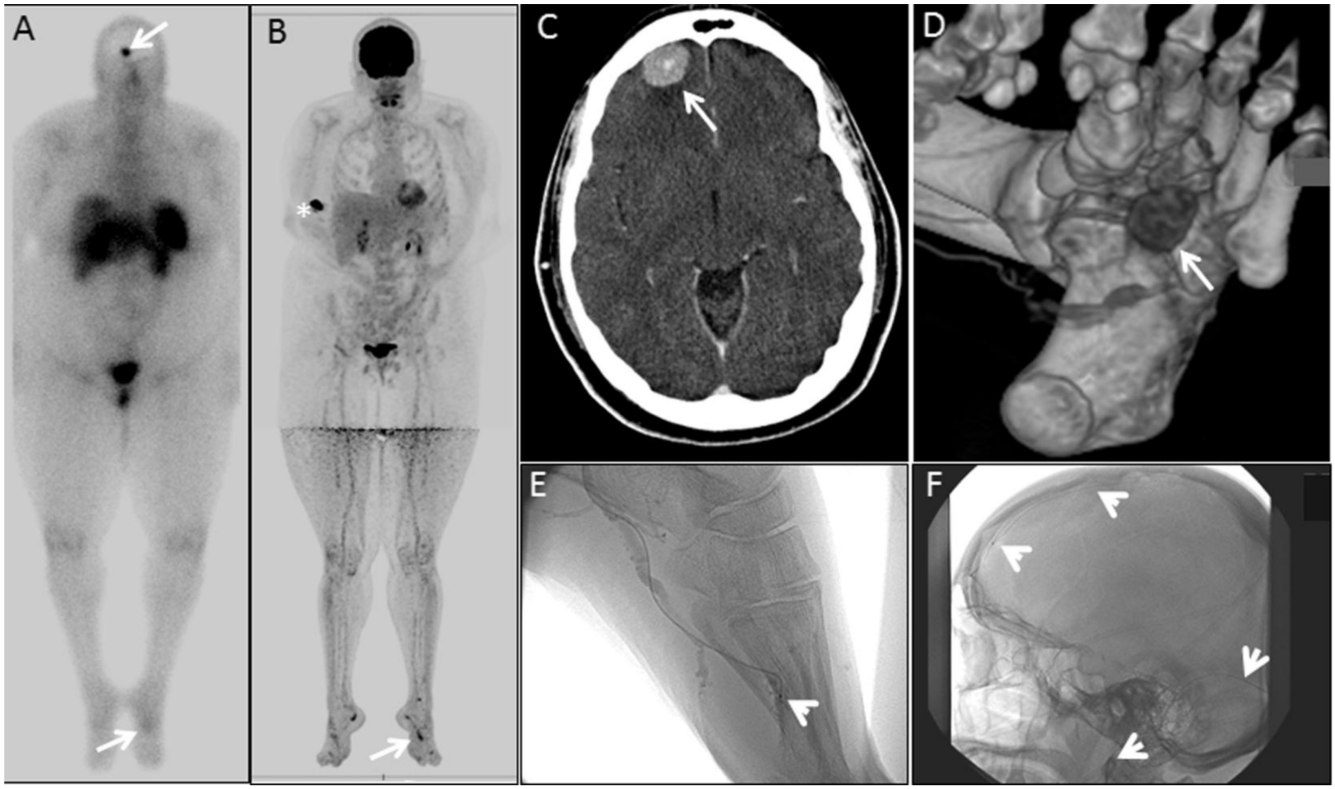

G

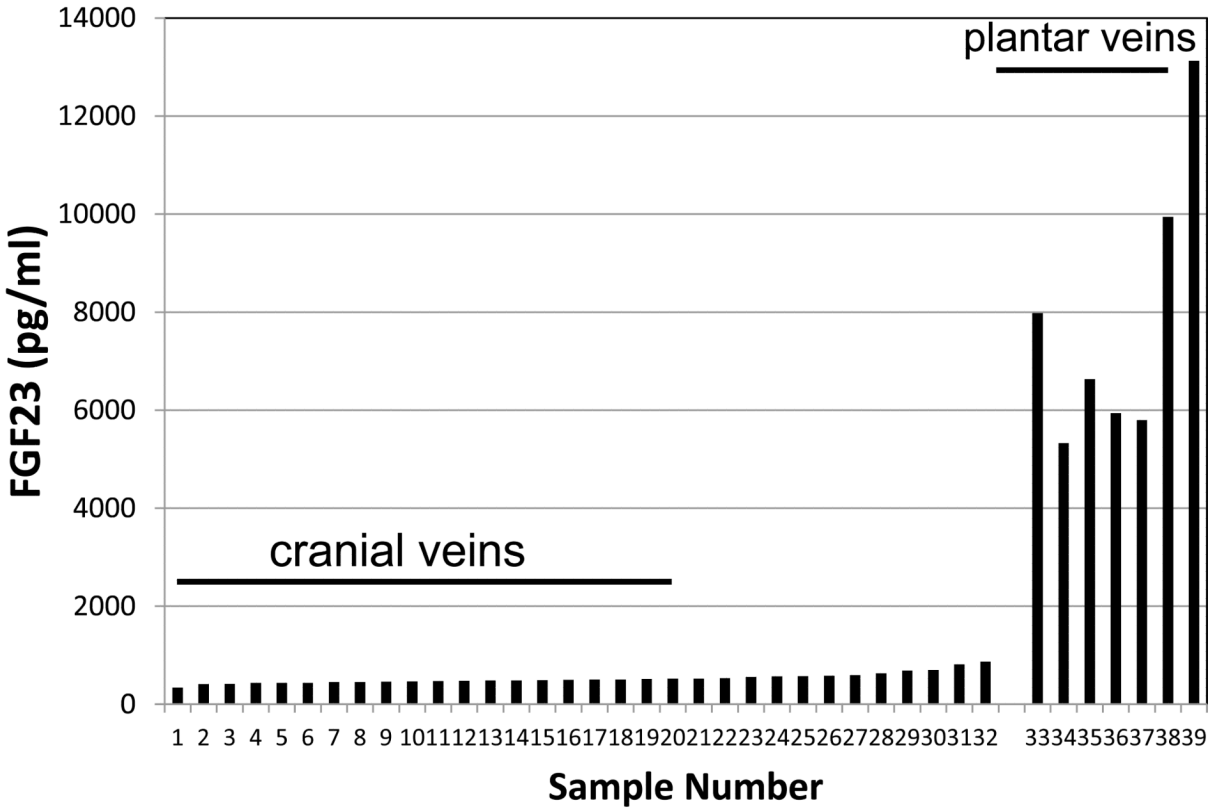

Figure 4.

An example of venous sampling in discriminating between two potential sites of tumor. Whole body octreo-SPECT was performed and identifed two suspicious lesions, white arrows (A). FDG-PET/CT suggested multiple lesions, including the lesion in the foot (B). The white asterisk (B) indicates the injection site. Anatomincal imaging studies confirmed the presence of a lesion at the brain-bone interface on CT scan (C), as well as a lesion on the plantar surface as shown on 3D CT scan (D). Venous sampling at these two sites was performed (E& F). In panels E & F, the course of the catheter the tips are indicated by white arrow heads. Measurement of intact FGF23 levels clearly revealed that the lesion in the foot was the source of the FGF23 (G).

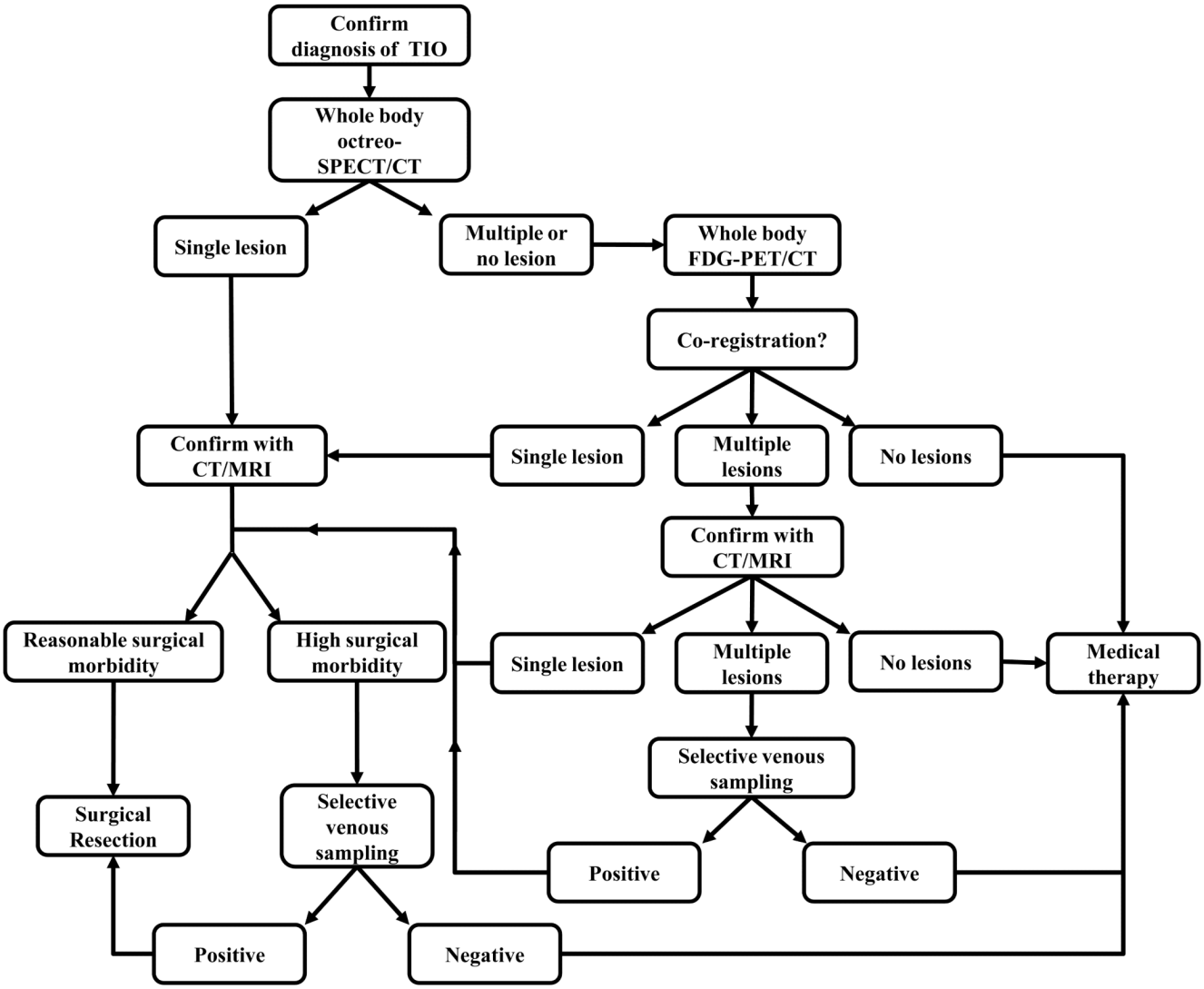

Figure 5.

Alogorithm for systematic approach to localizing tumors in tumor-induced osteomalacia. After confirming a clinical and biochemical picture of tumor-induced osteomalacia, we recommend obtaining functional imaging as a first step in tumor localization. Octreo-SPECT (SPECT/CT if available) is the recommended initial screening imaging test, as it was shown to have greater specificity and sensitivity than FDG-PET/CT. If a single lesion suspcious for TIO is found and it is confirmed on anatomical imaing and carries a reasonable surgical morbidity, surgical resection is recommended. If multiple lesions or no lesions are found on octreo-SPECT, FDG-PET/CT should follow. This may help to identify a lesion that was not initially seen on octreo-SPECT (as in Fig. 3), or help to confirm a lesion seen on octreo-SPECT. If appropriate, proceed to anatomical imaging with CT and/or MRI. If the area with the suspected lesion entails high surgical morbidity, or if multiple lesions are identified, selective venous sampling is recommended to confirm or rule out the tumor. If no lesion is found or a suspected lesion(s) is not confirmed on venous sampling, medical therapy is recommended.

Table 1

Subject Demographics

Subject No.	Gender	Age at Presentation	Phosphorus at Presentation	Intact FGF23 at Presentation	Disease-Related Complications
1	Female	29	1.5	1242	Pain, weakness, fractures[1], osteomalacia on biopsy
2[2]	Female	31	1.6	92	Rickets (childhood presentation), weakness, amputation[2]
3	Female	41	1.2	734	Pain, low bone mineral density[3]
4	Male	50	2	329	Weakness, fractures, ankle edema[4], muscle atrophy
5	Male	46	1.8	355	Fractures, falls
6[5]	Male	51	1.8	88	Pain, fractures, weakness
7	Male	61	1.6	890	Pain, fractures, osteomalacia on biopsy
8	Male	59	2	132	Pain, weakness
9	Male	50	1.6	1684	Pain, muscle atrophy, weight loss, osteomalacia on biopsy
10[6]	Male	46	1.2	84	Weakness, pain, fractures
11	Male	57	2.1	473	Pain, low bone mineral density
12	Male	50	1.6	119	Pain, weakness, gait abnormality, low bone mineral density
13	Male	39	1.8	1113	Ankle edema, pain, difficulty ambulating, fractures
14	Female	55	1.2	406	Fractures, pain, low bone mineral density
15	Male	44	1.6	353	Pain, fractures, stiffness, low bone mineral density
16	Male	44	1.8	95	Fractures, weakness, muscle atrophy
17	Male	33	2.2	146	Pain, weakness, fractures
18	Male	17	1.6	110	Pain, fractures, low bone mineral density
19	Male	37	1.8	290	Pain
20	Female	51	1.2	472	Weakness, pain
21	Female	47	1.9	1029	Pain, fractures
22	Female	62	2.0	156	Fatigue, pain, fractures, low bone mineral density
23	Male	67	1.4	1344	Pain, weakness, ankle edema, fractures, low bone mineral density
24	Female	18	1.4	76	Pain, weakness, myalgia, fractures, weight loss
25	Male	59	1.3	345	Pain
26	Female	14	1.6	177	Ankle edema, pain, fractures, weakness, muscle spasms

Subject No.	Gender	Age at Presentation	Phosphorus at Presentation	Intact FGF23 at Presentation	Disease-Related Complications
27	Male	57	2.1	294	Weakness, pain, falls, cramps, tetany
28	Female	66	1.6	2742	Falls, fractures, weakness, pain, fatigue
29	Male	48	2	482	Pain, fatigue, height loss
30	Female	49	1.9	535	Fractures, weakness, fatigue, pain, stiffness, gait abnormality
31[7]	Male	50	1.8	81	Fractures, fatigue, pain, muscle spasms, low bone mineral density
M:F	20:11		Reference Range: 2.5-4.8 mg/dl	Reference Range: 10-50 pg/ml	
Mean		48.5	1.7	337	
Median		47	1.69	546.4	
Range		14-67	1.2-2.2	76-2742	

[1] Most common fracture locations included ribs/clavicle, femur/pelvis, followed by back/vertebral compression fractures leading to height loss. Fractures were often characterized as “slow-healing”.

[2] Subject previously treated outside and presented to NIH with metastatic disease following persistent disease after amputation

[3] Low bone mineral density refers to either a Z-score of ≤ −2.0 when the study was performed at NIH or as reported in referral data.

[4] Ankle edema (bilateral or unilateral) was an unexplained, but surprisingly common finding among patients who otherwise had no evidence of heart failure or renal insufficiency.

[5] Subject previously treated outside, presented to NIH with recurrent disease, and eventually developed pulmonary metastases

[6] Subject previously treated outside and presented to NIH locally persistent

[7] Patient presented with clinical features consistent with Cowden syndrome however PTEN mutation testing was negative.

Table 2

Comparison of Octreo-SPECT and FDG PET/CT in localizing mesenchymal tumors in TIO.

	Tumor Positive	Tumor Negative	Total		
Octreo-SPECT positive	18	4	21	Sensitivity	0.95
Octreo-SPECT negative	1	7	9	Specificity	0.64
Total	19	11		PPV	0.82
				NPV	0.88
FDG PET/CT positive	14	7	21	Sensitivity	0.88
FDG PET/CT negative	2	4	6	Specificity	0.36
Total	16	11		PPV	0.62
				NPV	0.50

Octreo-SPECT, = ^{111}Indium-octreotide with single photon emission computed tomography FDG PET/CT = ^{18}fluorodeoxyglucose positron emission tomography/CT , PPV = positive predictive value, NPV = negative predictive value

Table 3

Results of localizing studies and tumor location

Localized:					
Subject Number	**Octreotide**	**FDG PET/CT**	**Venous Sampling**	**Tumor Location**	**Histopathological Diagnosis**
1	+	ND	_ [1]	Right maxilla	Infiltrative spindle cell and vascular lesion consistent with PMT
2	+	ND	ND	Left forearm with pulmonary metastases	Spindle cell sarcoma with focal collection of giant cells, consistent with PMT
3	+	ND	ND	Left ethmoid sinus	Hemangiopericytoma
5*	+	+	+	Left heel fat pad	PMT composed of spindle cells, clusters of osteoclast-like giant cells, and foci of cartilaginous metaplasia
6	+	+	ND	Right mandible with pulmonary metastases	Spindle cell tumor consistent with PMT (mandible); Features consistent with PMT and ameloblastic fibrosarcoma (metastases) (ref. 15)
10	+	+	ND	Left lateral femoral condyle	PMT
11 *	+	+	+	Left thigh	Angiolipoma with clear cells as well as pleomorphic features associated with PMT
13 *	+	+	+	Left fibula	Spindle cell neoplasm with features of PMT
14		+	_ [2]	T8 vertebral body	PMT (vertebral body tumor); atypical spindle and polygonal cells with enlarged, elongated nuclei and osteoclasts
15	+	+	+	Left acetabulum	Fragmented portions of bone showing spindle cell neoplasm highly suggestive of PMT
16	ND[3]	+	ND	Left lower back subcutaneous nodule	Tumor nodule in deep dermis comprised of spindle cells, vascular spaces, and bone formation consistent with PMT
19	+	+	+	Left greater trochanter	Focal spindle cell proliferation consistent with PMT
21 *	+	+	+	Left popliteal fossa	Epitheloid/spindle cell neoplasm consistent with PMT
22	+	−	+	Left frontal lobe intracranial mass	NA (not resected)
23	+	+	ND	Right proximal tibia	PMT, mixed connective tissue type
26	+[4]	+	+	Right periosteal nodule proximal tibia	Spindle cell neoplasm consistent with PMT
28	+	ND	ND	Left distal humerus periosteal-associated soft tissue mass	Spindle cell tumor with features of PMT

Localized:

Subject Number	Octreotide	FDG PET/CT	Venous Sampling	Tumor Location	Histopathological Diagnosis
29	+	+	+	Left lesser trochanter	Spindle cell lesion consistent with PMT
30	+	+	+	Left foot, plantar surface	Spindle cells and cartilaginous area with numerous osteoclast-like giant cells consistent with PMT
31	+	−	+	Right arm, volar aspect, just below elbow	[5]1-PMT; 2- PMT, mixed connective tissue variant; 3- lipoma; 4- hemangioma with lipomatous component and small portions of PMT in the periphery
No. Positive	18	14	11		
No. Negative	1	2	2		
No. Not Done	1	4	7		

Not Localized:

Subject Number	Octreotide	FDG PET/CT	Venous Sampling	Tumor Location	Histopathological Diagnosis
4	−	+	ND	NA	NA
7	+[6]	+	−	NA	NA
8	−	+	ND	NA	NA
9	+	+	−	NA	NA
12	−	−	ND	NA	NA
17	−	−	ND	NA	NA
18	+	+	+[7]	NA	NA
20	−	−	+[8]	NA	NA
24	+	+	−	NA	NA
25	−	−	ND	NA	NA
27	−	+	−	NA	NA
No. Positive	4	7	2		
No. Negative	7	4	4		
No. Not Done	0	0	5		

No. = number, + = positive study, - = negative study, ND = not done, NA = not applicable, * = subjects were positive control subjects in venous sampling study (Andreopoulou et al.), PMT = phosphaturic mesenchymal tumor

[1] Negative venous sampling performed as part of evaluation of recurrent disease. Not done at initial evaluation

[2] Needle aspiration of suspected lesion, venous sampling negative

[3] Tumor resected prior to performing octreo-SPECT.

[4] Lesion seen on octreo-SPECT only after identified on FDG-PET/CT

[5] Pleimorphic tumor with multiple distinct areas in a *PTEN* mutation negative patient who met clinical criteria for Cowden syndrome

[6] Surgery of lesion seen on octreotide did not result in resolution of disease. Lesion remained on post-operative anatomic imaging. Five year follow-up octreo-SPECT was negative

[7] Two suspicious sites on imaging. Venous sampling positive for one of two sites. Subject ultimately had surgery of both sites w/o resolution of disease

[8] Suspicious lesion identified on PET and venous sampling suggested that identified lesion was the source. Surgery was performed at an outside institution; pathology was consistent with enchondroma. Disease persisted post-operatively.